Received: 20 December 2020 | Revised: 1 June 2021 | Accepted: 14 July 2021 | Published on: 9 August 2021

DOI: 10.1002/joc.7310

RESEARCH ARTICLE

International Journal of Climatology RMetS

Recent evidence for warmer and drier growing seasons in climate sensitive regions of Central America from multiple global datasets

Iris T. Stewart[1,2] | **Edwin P. Maurer**[3] | **Kerstin Stahl**[2] | **Kenneth Joseph**[4]

[1]Department of Environmental Studies and Sciences, Santa Clara University, Santa Clara, California, USA

[2]Faculty of the Environment and Natural Resources, University of Freiburg, Freiburg im Breisgau, Germany

[3]Department of Civil, Environmental, and Sustainable Engineering, Santa Clara University, Santa Clara, California, USA

[4]Department of Bioengineering, Santa Clara University, Santa Clara, California, USA

Correspondence
I. T. Stewart, Department of Environmental Studies and Sciences, Santa Clara University, 500 El Camino Real, Santa Clara, CA 95053, USA.
Email: istewartfrey@scu.edu

Funding information
Deutsche Forschungsgemeinschaft, Grant/Award Number: STA 632/6-1; Frias Institute of Advanced Studies (FRIAS); National Science Foundation, Grant/Award Number: BCS-1539795

Abstract

Smallholder livelihoods throughout Central America are built on rain-fed agriculture and depend on seasonal variations in temperature and precipitation. Recent climatic shifts in this highly diverse region are not well understood due to sparse observations, and as the skill of global climate products have not been thoroughly evaluated. We examine the performance for several reanalysis and satellite-based global climate data products (CHIRPS/CHIRTS, ERA5, MERRA-2, PERSIANN-CDR) as compared to the observation-based GPCC precipitation dataset. These datasets are then used to evaluate the magnitude and spatial extent of hydroclimatic shifts and changes in aridity and drought over the last four decades. We focus on water-limited regions that are important for rain-fed agriculture and particularly vulnerable to further drying, and newly delineate those regions for Central America and Mexico by adapting prior definitions of the Central American Dry Corridor. Our results indicate that the CHIRPS dataset exhibits the greatest skill for the study area. A general warming of 0.2–0.8°C·decade^{-1} was found across the region, particularly for spring and winter, while widespread drying was indicated by several measures for the summer growing season. Changes in annual precipitation have been inconsistent, but show declines of 20–25% in eastern Honduras/Nicaragua and in several parts of Mexico. Some regions most vulnerable to drying have been subject to statistically significant trends towards summer drying, increases in drought and aridity driven by precipitation declines, and/or a lengthening of the winter dry season, highlighting areas where climate adaptation measures may be most urgent.

KEYWORDS

Central America, climate change, drought, dry corridor, precipitation

1 | INTRODUCTION

Central America (CA) is a region particularly vulnerable to climate disruption expected from global warming, with Honduras, Nicaragua, and Guatemala ranked in the 10 countries considered most at risk (Kreft *et al*., 2013). Throughout CA, 90% of agricultural production is rainfed, resulting in a high dependency on rainfall for food production, biodiversity, and soil preservation (Wani *et al*., 2009). In addition, growing-season temperatures are important, as the production of principal crops is expected to decline with rising temperatures (Hannah *et al*., 2017). Smallholder farmers routinely face threats to their livelihoods by pricing and economic structures, climatic variability and extremes, and crop diseases (Avelino *et al*., 2015; Hannah *et al*., 2017), and as a result, possess limited adaptive capacity. Thus, information on climate variability and change provides context and supports building sound adaptation strategies and adaptive capacity at the local scale.

The unique geography of CA and the sparse availability of ground observations for climatic variables provide considerable challenges for assessments of climatic variability and change (Carvalho, 2020). Complex topography of volcanic origin shapes a narrow isthmus located between the two dynamic oceanic systems of the Pacific and Atlantic Oceans (Pérez-Briceño *et al*., 2016). The migration of the Inter Tropical Convergence Zone (ITCZ) and the associated changes in strength of the trade winds drive the timing of the seasons, the distinct seasonality in precipitation for much of the area, and sensitivity to climate change (Hidalgo *et al*., 2015; Maldonado *et al*., 2018). The complex interactions between topography and climate systems occur on spatial scales not well represented in global models, but improvements have been made with dynamical downscaling driven by regionally coupled atmosphere–ocean models (Cabos *et al*., 2019) and through regional modelling (i.e., Hannah *et al*., 2017), yet regional modelling is not able to represent the entire study area in near-real-time. At interannual scales, the El Nino/Southern Oscillation (ENSO) is the main climate modulator (Maldonado *et al*., 2018) and much concern from farmers regarding floods and droughts is associated with ENSO events.

Given the regional complexity and scarcity in observational data, our study encompasses three objectives: We (a) test the performance of high-quality satellite and reanalysis datasets for the region, (b) evaluate the consistency of recent hydroclimatic trends for temperature, precipitation, drought, and aridity, and (c) delineate climate-sensitive regions based on metrics established for the Central American Dry Corridor (CADC) and identify if and where these regions have become drier.

1.1 | Climate-sensitive regions

The CADC is a comparatively arid region within CA with a heightened susceptibility to drought and drought impacts (Pennington and Ratter, 2006; Pérez-Briceño *et al*., 2016; Gotlieb *et al*., 2019). Varying definitions of the CADC agree about its location on the Pacific side of CA extending from western Guatemala through northern Costa Rica, with some studies including the Dry Arc (Arco Seco) of Panama (Gotlieb *et al*., 2019). However, a generally recognized objective delineation of the CADC is elusive. Most metrics to define the extent of the CADC include climatic indices, such as those employed by the International Center for Tropical Agriculture (CIAT) that defined the CADC as prone to drought based on their Climate Risk Index calculated from consecutive dry months (Quesada-Hernandez *et al*., 2019). A study by the Food and Agriculture Organization (FAO) of the United Nations (van der Zee Arias *et al*., 2012) identified both a climatic and an ecological basis for the CADC. Ecologically, the CADC encompasses tropical dry forest ecosystems that stretch from Chiapas in Mexico to near Guanacaste in Costa Rica. Climatically, it is subject to recurring droughts and defined by an annual dry season of 4–6 months, low to medium precipitation, and low evapotranspiration. A 2019 consensus statement uses both socioeconomic and climatic indices to define the CADC, including a drier climate than in other areas of CA, a marked winter dry season of at least 4 months, bimodal precipitation patterns with peaks in June and September (Magaña *et al*., 1999), and high variability in rainfall that is tied to ENSO (Gotlieb *et al*., 2019). Quesada-Hernandez *et al*. (2019) propose a dynamic extent of the CADC for wet, dry, and average conditions in a CA core region, using a 1979–1999 meteorological station network biased towards the Pacific side of the isthmus.

In addition to climatic characteristics, the CADC is recognized as a rural area with rich biodiversity (Pennington and Ratter, 2006) and a high prevalence of subsistence farming and economic vulnerability (van der Zee Arias *et al*., 2012; Gotlieb *et al*., 2019). Within the CADC, the impacts of droughts, floods, and extreme precipitation on crops and livelihoods have been particularly severe (Pérez-Briceño *et al*., 2016). Although extended dry seasons and a highly seasonal distribution of rainfall have been named as characteristics of the CADC, they have so far not been included in delimitations.

1.2 | Precipitation and temperature data

An increasing number of global climate products have been developed at progressively finer spatial and temporal

resolution and can aid to overcome sparse spatial coverage of on the ground meteorological data. These products have been used extensively for hydrologic applications (Cavazos *et al*., 2020), and early drought warning systems (Funk *et al*., 2019). Their advantage lies in the spatially and temporally complete coverage that is consistent with larger synoptic processes, and, for many products, is corrected by local observations. A number of studies have evaluated the performance of these datasets for particular regions, identifying some of the difficulties in capturing local variability at larger spatial scales (Sun *et al*., 2018; Beck *et al*., 2019; Zhao and Ma, 2019; Chen *et al*., 2020), and the spatiotemporal variability of precipitation under complex geographic conditions (Sun *et al*., 2018; Beck *et al*., 2019; Chen *et al*., 2020). In addition, precipitation product performance was strongly tied to the spatial coverage of surface stations, satellite algorithms, and data assimilation models. Inconsistencies between these limit the capability of the products for climate monitoring, attribution, and model validation (Sun *et al*., 2018). Thus, the relative performance of available datasets is to some degree a function of topographic complexity, climate regime, season, and network station density, and results cannot be extrapolated to other regions (Sun *et al*., 2018; Beck *et al*., 2019; Chen *et al*., 2020). In spite of its socio-economic vulnerability and sparse observational data, the CA isthmus has not been the focus of a performance evaluation of global data products to date.

1.3 | Hydroclimate changes

Both drought and aridity threaten the productivity of rainfall agriculture and the livelihoods of smallholder farmers globally, including in many regions of CA. Drought refers to a temporary reduction in water availability compared to a long-term climatological mean, while aridity refers to a prolonged state of water limitation (Greve *et al*., 2019). Impacts of drought are likely to be particularly severe in water-limited regions. Changes in drought and aridity are key effects expected from global warming, and thus important considerations for assessments of hydroclimatological changes. Evaluations of drought and aridity depend on a description of the complex interactions of energy and terrestrial water fluxes, parameters that are rarely available in practice; thus, more simplified indices are widely used.

End-of-century projections of climatic changes from GCMs over CA suggest warming of surface air temperatures of 3–4°C and significant decreases in precipitation, increasing the aridity of the region (Karmalkar *et al*., 2011; Hidalgo *et al*., 2013). As temperature and precipitation changes in other global regions have been attributed to anthropogenic drivers, including CA (Marvel *et al*., 2019), an important question is whether evidence for projected hydroclimatic shifts can be discerned in the climatic record to date.

Prior work on recent hydroclimatic trends for CA has used both station observations and global products but has not included the most recent decade. Robust warming of more than 0.3°C/decade throughout CA and Mexico for the latter 20th and early 21st century, with some indications for local cooling over Honduras and northern Panama, has been identified (Hidalgo *et al*., 2017; Alfaro-Córdoba *et al*., 2020; Cavazos *et al*., 2020). Changes in precipitation have been inconsistent in direction and magnitude, of lower significance, hampered by the lack of on-the-ground monitoring, and dependent on the data base used (Hannah *et al*., 2017; Hidalgo *et al*., 2017; Muñoz-Jiménez *et al*., 2019; Cavazos *et al*., 2020). Cavazos *et al*. (2020) found precipitation decreases over the 1980–2010 period for the GPCP and CHIRPS datasets, with increases for Era-Interim and CRU. Trend analysis on 5-km gridded monthly climate fields built from station and reanalysis data for the 1970–1999 period indicated little evidence for significant precipitation trends (Hidalgo *et al*., 2017).

While prior studies have consistently reported significant warming, they have not identified a decrease in water availability resulting from either warming or changes in precipitation. Multiple explanations for the lack in observed precipitation changes are plausible: near-term projections of precipitation changes from large-scale GCMs may be biased; warming to date may not have been sufficient to drive aridity or precipitation changes; or the data products available are not sufficient in temporal and spatial coverage or accuracy. Even without any significant changes to precipitation, the observed widespread warming may impact water flows and availability, as increases in temperature drive increases in both evapotranspiration and aridity, as well the frequency and magnitude of drought. To explore this possibility, Alfaro-Córdoba *et al*. (2020) used the 1970–1999 observational dataset by Hidalgo *et al*. (2017) and found that warming had, contrary to expectations, mostly not been sufficient to drive concurrent and significant changes in aridity, except in locations of Costa Rica and Nicaragua. The analysis by Hidalgo *et al*. (2017) did not include the most recent decade, globally recognized as the warmest on record.

In summary, studies on hydroclimatic variability and change in CA to date have used historic datasets that have not included the most recent decade (Hidalgo *et al*., 2017; Alfaro-Córdoba *et al*., 2020), when global temperatures have been the warmest (NOAA National Centers for Environmental Information, 2020), and

during which a widespread and severe drought event affected critical areas of the region (ReliefWeb, 2020). Thus, they have not reflected the changes that have taken place to date. In addition, recent available data products have not been compared with a focus on the study region. In response, we examine which of the climatic datasets available for CA would be appropriate to use for the study area in the absence of a comprehensive network of monitoring stations; what hydroclimatic shifts have occurred in the area over the past four decades; and whether and where globally observed warmer surface air temperatures have driven increases in drought and aridity in the region. Finally, we seek to identify vulnerable regions in CA based on previously established definitions on what constitutes the CADC and assess in what ways any hydroclimatic shifts are intersecting with these regions.

2 | METHODS

The study region consists of CA and its bordering regions with North America, South America, and the Caribbean, and is bound by 0–25 N latitude and 105–75°E longitude, including countries from southern Mexico to northern Colombia, and Cuba (Figure 1). The regions beyond those considered CA were included to observe the continuity and/or boundaries of any hydroclimatic changes between the CA isthmus and the land masses of North and South America. We begin our study with an intercomparison of different data products to determine whether one rises above the others in quality for the region and variables of this study, and to gauge the variability among the datasets. To identify areas of particular climatic sensitivity we develop the delimitation of a region based on climatic characteristics identified for the CADC, and using the highest performing datasets from the comparison in this study. We then quantify the magnitude and spatial and temporal extent of hydroclimatic shifts, with a focus on the climate sensitive regions defined above, and most recent data. Finally, we reassess whether warmer temperatures to date have driven greater aridity in the region by including in the computation the most recent period to establish changes in aridity and the length of the dry season, and by comparing trends in the daily precipitation-based standard precipitation index (SPI) with those of the standard precipitation and evapotranspiration index (SPEI), which includes temperature.

In the absence of available station data, we used the Global Precipitation Climatology Center (GPCC) as a benchmark for comparison. The GPCC dataset represents the most comprehensive global collection of daily and monthly precipitation from in situ climate stations. We relied on the GPCC Full Data Daily Product V.2018, which is based on near- as well as non-real-time data from more than 35,000 stations (Schneider *et al.*, 2018; Ziese *et al.*, 2018) as our observation standard. It is available at a 1.0° spatial resolution, but was resampled using conservative remapping to the same 0.25° grid used for

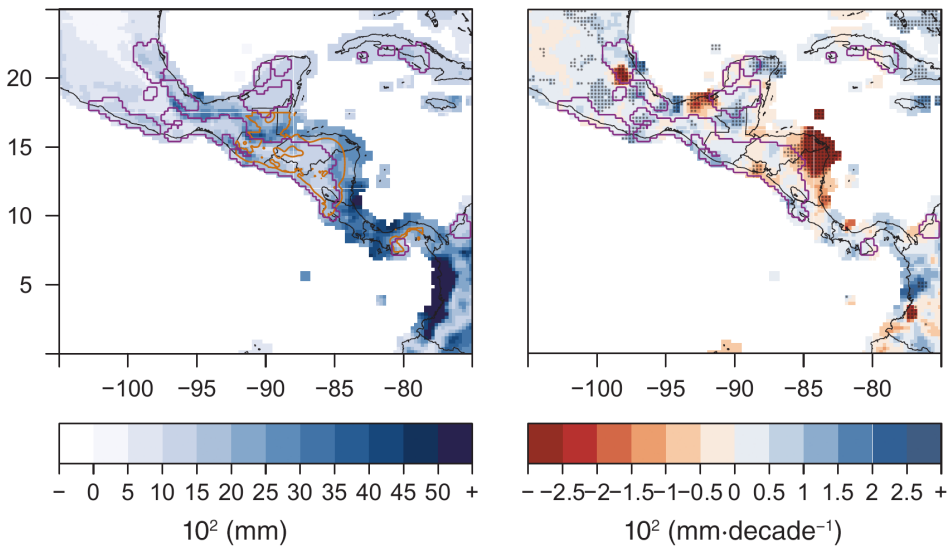

FIGURE 1 Mean annual precipitation in the study region (left panel) and trends in annual precipitation over the 1982–2016 period for the GPCC reference dataset (right panel). Statistically significant areas marked with dark shading. Dark orange boundaries indicate the spatial extent of the Central American Dry Corridor (CADC) as determined by dynamic delimitation for average conditions by Quesada-Hernandez *et al.* (2019), and magenta coloured boundaries indicate the delimitation of vulnerable regions based on CADC definitions as developed by this study [Colour figure can be viewed at wileyonlinelibrary.com]

all intercomparisons between datasets. Conservative remapping is an interpolation technique designed to maintain the energy and water budgets between the raw and interpolated fields (Jones, 1999; Hanke *et al*., 2016).

The global model and satellite based datasets compared to the GPCC were selected for their finer spatial resolution, temporal depth, coverage of the study region, as well as their performance in evaluative studies (Beck *et al*., 2019) for regions where robust station networks exist. Each was aggregated to the same 0.25° grid as the GPCC data if at a finer native spatial resolution. Characteristics for these datasets are described below and in Table 1. There are many additional satellite-based, reanalysis, and observationally derived datasets that could have been included in this study (e.g., Mesinger *et al*., 2006; Harris *et al*., 2020; Tang *et al*., 2020). In addition to the considerations noted below, our focus was on global datasets that provided daily data, and we restrict our analysis to the climate over the past four decades, for which satellite data are available. Our aim is not an exhaustive evaluation of all available datasets but a characterization of the uncertainty among four commonly used datasets to help frame more in-depth results conducted with any one dataset. The inclusion of additional datasets or the use of a different time period of evaluation could change the results.

The Modern-Era Retrospective Analysis for Research and Applications (MERRA-2) dataset represents the latest atmospheric reanalysis product by NASA's Global Modeling and Assimilation Office (Gelaro *et al*., 2017; Reichle *et al*., 2017b). We used the corrected precipitation from MERRA-2, which includes the assimilation of precipitation observations and applies a number of other corrections (Reichle *et al*., 2017a; 2017b). The European Centre for Medium-Range Weather Forecasts (ECMWF) Reanalysis, version 5 (ERA-5) data are the widely used high-performing fifth-generation reanalysis product by the Copernicus Climate Change Service (C3S) at the ECMWF (Beck *et al*., 2019; Hersbach *et al*., 2020). ERA-5 provides hourly estimates of atmospheric, land, and oceanic climate variables. We used daily total precipitation and mean surface air temperature data (Albergel *et al*., 2018; Beck *et al*., 2019). The NCAR/UCAR Precipitation Estimation from Remotely Sensed Information using Artificial Neural Networks – Climate Data Record (PERSIANN-CDR) dataset provides daily rainfall estimates produced using the PERSIANN algorithm on infrared satellite data, and the training of the artificial neural

TABLE 1 Overview of the gauge-corrected (quasi-)global daily gridded datasets compared for the Central American study region

Name	Details	Data source(s)	Native spatial and temporal resolution	Temporal and spatial coverage	Variables used	Primary reference
GPCC V.2018	Global Precipitation Climatology Center	G	1° × 1° (~12,500 km^2)	1982–2016 global	pr	Schneider *et al*. (2018)
MERRA-2	Modern-Era Retrospective Analysis for Research and Applications 2	G, S, R	~0.5° × 0.5°, 50 km^2 hourly	1980–NRT global	pr corr, tas	Global Modeling and Assimilation Office (GMAO) (2015)
ERA-5	European Centre for Medium-Range Weather Forecasts Reanalysis, V5	G, R	30 km^2	1979– NRT global	pr, tas	Copernicus Climate Change Service (C3S) (2017)
PERSIANN-CDR	Precipitation Estimation from Remotely Sensed Information using Artificial Neural Networks Climate Data Record	G, S	0.25° × 0.25° (~800 km^2) daily	1983–2016 quasi-global, 60° N/S	pr	Sorooshian et al. and NOAA CDR Program (2014)
CHIRPS V2.0	Climate Hazards group InfraRed Precipitation with Stations V2.0	G, S, R, A	0.05° × 0.05° (~25 km^2) daily	1981–NRT land, quasi-global, 50° N/S	pr	Funk *et al*. (2014)
CHIRTS	Climate Hazards group InfraRed Temperature with Stations	G, S, R	0.05° × 0.05° (~25 km^2)	1983–2016 (quasi-global, 60°S–70 N)	tas	Funk *et al*. (2019)

Abbreviations: A, analysis; G, gauge; global, fully global coverage, including ocean areas; land, coverage is limited to the terrestrial surface; NRT, near-real time; quasi-global, coverage that extends to the high latitudes; R, reanalysis; S, satellite.

network based on the National Centers for Environmental Prediction (NCEP) stage IV hourly precipitation data. The PERSIANN-CDR is adjusted using the Global Precipitation Climatology Project (GPCP) v2.2 product, generated by merging microwave, infrared, and sounder data and precipitation station data (Ashouri *et al*., 2015; 2016). The Climate Hazards group Infrared Precipitation with Stations (CHIRPS) v.2.0 dataset is developed by the Climate Hazards Group (CHG) at the University of California, Santa Barbara and the U.S. Geological Survey Earth Resources Observation and Science Center. Daily, monthly, and seasonal products are built around blending satellite Cold Cloud Duration (CCD) observations and improved interpolation techniques of high resolution, long period-of-record precipitation estimates. CHIRPs forms the basis for the U.S. Agency for International Development's Famine Early Warning Systems Network (FEWS NET), with the largest focus in Africa. Daily temperatures are available through the Climate Hazards Center Infrared Temperature with Stations (CHIRTS) dataset at the same high spatial resolution as CHIRPS, and are derived from combining long high-resolution cloud-screened archives of geostationary satellite thermal infrared (TIR) with stations observations (Funk *et al*., 2019) adjusted using temperature data from ERA-5.

The datasets selected for this study are some of the highest performing for uncorrected (ERA5) and corrected (MERRA-2 and CHIRPS) datasets in regional comparison studies (Sun *et al*., 2018; Beck *et al*., 2019; Zhao and Ma, 2019). CHIRPS has demonstrated higher correlations, and less bias and mean absolute errors with GPCC than several other datasets, and has served well for near-real-time drought monitoring (Peterson *et al*., 2015). At the same time, the GPCC product used in this study is considered adequately independent of the CHIRPS dataset where GPCC is routinely used as a baseline against which CHIRPS or other products based on remote sensing are compared (i.e., Funk *et al*., 2015). PERSIANN-CDR has performed well for long-term historical drought analysis and capturing the temporal variability of the intensity and amount of precipitation extremes on global scales (Zhao and Ma, 2019; Chen *et al*., 2020). Significant uncertainties in both modelling and rainfall observation are especially pronounced in the lower latitudes (Sun *et al*., 2018). These studies have underscored that all types of observational-based rainfall products have strengths and weaknesses and that the selection of dataset(s) must be carefully weighed with respect to their application (Nogueira, 2020).

The performance of all reanalysis and remotely sensed precipitation datasets in this study was evaluated against the GPCC interpolated station data at each grid cell over land using the Kling-Gupta efficiency (KGE) measure. KGE scores facilitate the analysis of the relative importance of different components (correlation, bias, and variability) in a goodness-of-fit analysis. It is well-established for the intercomparison of global datasets (Beck *et al*., 2019). KGE scores were not evaluated for surface temperature, as no comparable reference dataset was available. KGE is defined (Gupta *et al*., 2009; Kling *et al*., 2012) as

$$\mathrm{KGE}=1-\sqrt{(r-1)^2+(\beta-1)^2+(\gamma-1)^2},$$

where the correlation component r is represented by Pearson's correlation coefficient, the bias component β by the ratio of estimated and observed means, and the variability component γ by the ratio of the estimated and observed coefficients of variation. Thus,

$$\beta=\frac{\mu s}{\mu o}\text{ and }\gamma=\frac{\frac{\sigma s}{\mu s}}{\frac{\sigma o}{\mu o}},$$

where μ and σ are the distribution mean and standard deviation, and the subscripts s and o indicate estimate and reference, respectively. KGE, r, β, and γ all have their optimum at unity. KGE was calculated and mapped using daily values for the 1983–2016 period, for which all datasets overlap. Median and interquartile ranges for KGE value distributions by country were then determined to evaluate regional differences and provide guidance for practical applications. For each dataset, median values for the r, β, and γ statistics were calculated and compared to determine the most important contributing factor(s) to a high KGE score.

A spatial delineation for vulnerable regions within the study area was developed following the CADC precipitation characteristics reported by Gotlieb *et al*. (2019), which summarized a workshop consensus statement from Central American researchers. Gotlieb *et al*. (2019) noted a highly seasonal climate, drier than in the remainder of the continent, with a summer wet season that includes a mid-summer drought and frequent dry spells, a well-defined and long dry season of at least 4 months in boreal winter, and a relationship to the ENSO phenomenon such that El Niño conditions are connected to drying. To translate those descriptions into numeric terms, we identified all cells in the study region where, based on the CHIRPS precipitation dataset and averaged over the 1981–2019 period, the following conditions were met:

1. Average annual precipitation was >800 and <2,000 mm·year^{-1}.

2. Average wet season (May–September) mean fractional precipitation was >60%, and dry season (January–April) mean fractional precipitation <15% of mean annual precipitation totals.
3. The length of the average annual dry season, calculated from twice smoothed daily data, and defined as daily precipitation <2.5 mm exceeds 120 days.
4. The monthly Ocean Niño Index (ONI; NOAA, 2020) and monthly precipitation were correlated such that above normal temperatures in the 3-month running mean of ERSST.v5 SST anomalies in the Niño3.4 region correspond to decreases in precipitation.

The area thus determined was mapped in comparison to that proposed by Quesada-Hernandez *et al*. (2019) and served to identify areas with high sensitivity to drying across the study region. The FAO approach to identifying the CADC included all areas where there is a dry season of at least 4 months, but few details on either the dataset or the calculations are given and no geospatial dataset of this area is available.

As measures of hydroclimatic changes, we computed annual and seasonal trends for daily average surface temperature (ERA5, MERRA-2, CHIRTS datasets), and daily precipitation (GPCC, CHIRPS, ERA5, MERRA-2, PERSIANN-CDR datasets) over the period for which each dataset was available. Trends were determined using the rank-based, nonparametric Mann–Kendall (MK) test (Mann, 1945; Kendall, 1948; Sen, 1968; Siegel, 1982). In addition, we calculated the percentage difference in the means between annual and seasonal average precipitation and the difference in the mean annual temperature between the first (1999 and earlier) and second (2000 and later) part of the study period. The statistical significance in the differences of the means were calculated by the Wilcoxon signed-rank test (Wilcoxon, 1945), a nonparametric alternative to paired *t* tests when data are not normally distributed. A significance level of $\sigma = 0.05$ is used for all statistical tests. Results were compared between datasets and regions within the study area, with a particular focus on the vulnerable regions that fulfil CADC conditions that were identified as described above.

To assess whether the warmer temperatures and precipitation changes to date have driven changes in drought and aridity indices in the region we relied on quantifying changes in four metrics: (a) the number of days with Standardized Precipitation Index (SPI) (McKee *et al*., 1993) values indicating drought conditions, DD_{SPI}, and (b) the number of days with the Standardized Precipitation-Evapotranspiration Index (SPEI) (Vicente-Serrano *et al*., 2010) indicating drought, DD_{SPEI}, (c) the length of the annual dry season (L_{DS}), and (d) the aridity index (AI). All indices were calculated using CHIRPS precipitation data and are described in greater detail below.

The SPEI and the AI describe the interaction between temperature and precipitation and require potential evapotranspiration (PET). Daily PET was calculated following the Penman–Monteith approach and based on CHIRPS precipitation and ERA-5 temperature data. While this method requires additional input of net radiation and humidity, an iterative algorithm for estimating these inputs has been developed (Kimball *et al*., 1997; Thornton and Running, 1999) and is implemented in the METSIM software (Bennett *et al*., 2020) employed in this study.

Both SPI and SPEI are computed similarly, by summing precipitation (SPI) or water balance anomalies (SPEI), expressed as the difference between precipitation and PET, over a prescribed time scale (31 days for this study). The accumulated values are transformed to a normalized index using parametric probability distributions. SPI/SPEI calculations were based on the SCI R package developed by Stagge *et al*. (2015), as adapted to work with daily data, and using their recommended probability distributions for normalizing the indices. Both SPI and SPEI values of −1 correspond to the 16th percentile, with values below −1 indicating moderate to exceptional drought conditions (Heim, 2002). We compared July–August DD_{SPI} and DD_{SPEI} trends for the 1981–2018 period to those of the drier part of the year (November–April). July and August fall within the summer wet season, but include also the time of the midsummer drought, a period of reduced rains that is important to the planting cycle, and has historically taken place between July 15 and August 15. Concerns over the changes in the midsummer drought with climate change have been noted (Anderson *et al*., 2019; Quesada-Hernandez *et al*., 2019). Furthermore, to distinguish the relative potential contributions of warmer temperatures and decreases in precipitation to changes in drought, we removed the linear temperature trends (removing trends for each month independently) and re-calculated PET with this detrended data.

The L_{DS} metric was determined as the maximum length of continuous dry days during the October–June annual dry season, using twice-smoothed daily data. Dry days were defined as those with less than 2.5 mm of precipitation after smoothing. Precipitation thresholds for a "dry day" in the literature range from 0.1 to 10.0 mm·day^{-1} (Liu *et al*., 2015), in substantially different climates. The value of 2.5 mm used here is close to that employed by (McCabe *et al*., 2010) for the seasonal and semi-arid southwestern United States.

The AI was calculated on monthly and yearly time scales as the ratio of precipitation to potential evapotranspiration given by

$$\mathrm{AI} = \frac{P}{\mathrm{PET}},$$

where AI is the aridity index, P precipitation (mm), and PET the potential evapotranspiration (mm). This definition of AI is consistent with many authoritative references (e.g., Mirzabaev *et al*., 2019) though its inverse is also common in other studies (e.g., Greve *et al*., 2019).

Changes in the DD_{SPI}, DD_{SPEI}, L_{DS}, and AI metrics were analysed using Mann–Kendall trend and the Wilcoxon signed-rank tests, as described above.

Finally, to identify where drying has taken place within particularly vulnerable areas, we identified all areas within the climate sensitive regions for which statistically significant trends towards drying in either mean annual precipitation, summer wet season (JJA) precipitation, winter dry season (DJF) precipitation, or July aridity were found.

3 | RESULTS

The strong geographic and hydroclimatological variability of CA and its bounding regions is reflected in the wide range in mean annual precipitation, from <50 mm in the dry highlands of Mexico, to >4,000 mm over the wet lowlands of Nicaragua, Costa Rica, and Panama (Figure 1). Changes in the annual precipitation for the reference GPCC dataset were variable, and most areas did not exhibit statistically significant trends. Exceptions included areas of both significant increases and decreases in annual precipitation in Mexico, and a large area with significant decreases on the Atlantic side of Nicaragua and Honduras. Figure 1 compares the delimitation of the CADC by the dynamic approach of Quesada-Hernandez *et al*. (2019) for normal conditions, and the delimitation of climate-sensitive regions based on CADC criteria by this study. In core areas for Guatemala, Honduras, El Salvador, Nicaragua, and Panama, there is much overlap between these outlines. Main differences between the delimitations are centred on the areas outside of the Guatemala-Panama region, where conditions similar to those of the CADC exist and where the outline of climate-sensitive regions developed for this study identifies areas with highly seasonal climates, limited rainfall, and high vulnerability to drying similar to those of the CADC. These climate-sensitive areas include regions of southern Mexico, Cuba, and Colombia. The spatial extent by Quesada-Hernandez *et al*. (2019), by contrast, includes more of the wetter, Atlantic region, and also excludes all areas north of the Guatemalan border. Two out of the three regional-scale areas with statistically significant trends towards drying overlap at least partially with the vulnerable areas as identified in this study (Figure 1).

Evaluation of the KGE performance indicator scores suggests that all precipitation datasets derived from satellite and reanalysis data (CHIRPS, ERA5, MERRA-2, PERSIANN-CDR) perform reasonably well as compared to the purely observation-based GPCC data (Figures 2 and 3). KGE scores range from 0.2 to 1.0 for almost all regions and for all datasets. The northern part of the study region, mainly Mexico, is generally a better fit with GPCC than the southern part, comprising Honduras, Nicaragua, Costa Rica, and Panama. Considering the median and the interquartile ranges of the KGE values by country, the CHIRPS dataset achieved the consistently highest scores along the entirety of the CA isthmus. The MERRA-2 dataset performance exhibited the largest differences between northern and southern regions of all the datasets and was the highest performing dataset for the northernmost region. A comparison of the individual KGE statistics indicated that the CHIRPS dataset, for which r, β, and γ were closest to the ideal value of 1, performed best of all datasets compared, while the MERRA-2 dataset achieved the lowest scores for the region as a whole (Table 2). Generally, the values of

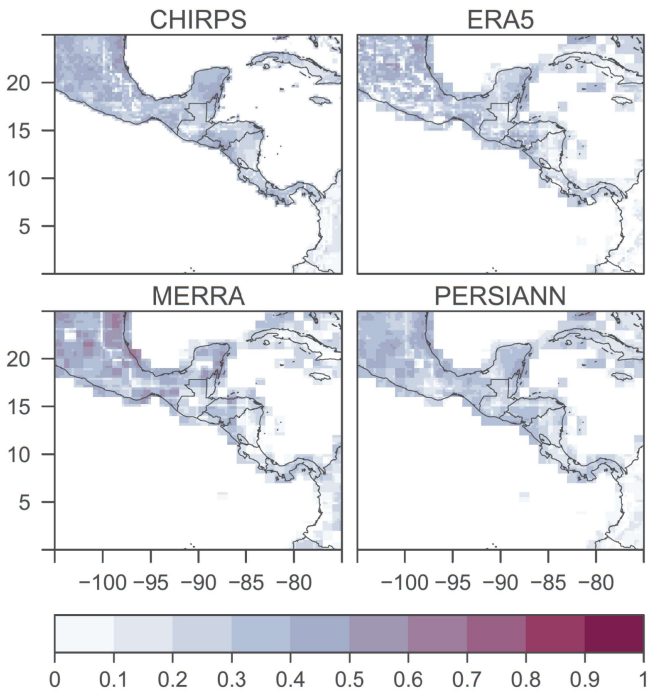

FIGURE 2 The KGE index evaluated between precipitation datasets used for evaluation and the GPCC reference dataset [Colour figure can be viewed at wileyonlinelibrary.com]

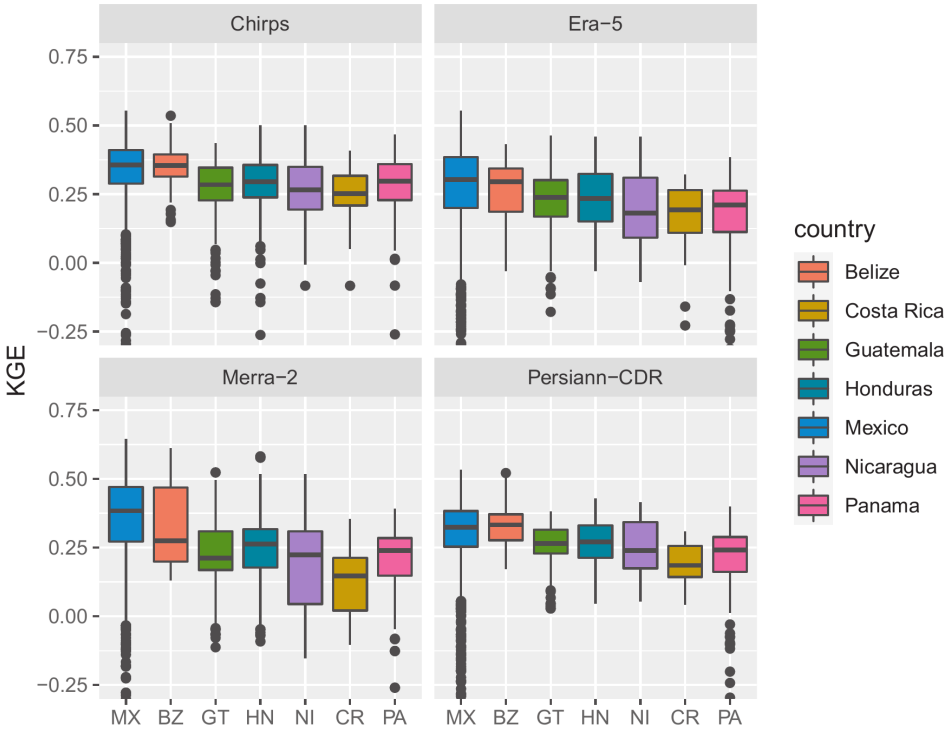

FIGURE 3 Medians and interquartile ranges for KGE index value distributions by country (north to south) and dataset under consideration [Colour figure can be viewed at wileyonlinelibrary.com]

TABLE 2 Median values of the individual components making up the Kling-Gupta efficiency (KGE), comparing Pearson's correlation coefficient (r), the ratio of estimated and observed means (β), and the ratio of the coefficient of variation (γ) for each dataset and across the study region

Statistic/dataset	CHIRPS	ERA-5	MERRA-2	PERSIANN-CDR
r	0.82	0.71	0.68	0.74
β	0.80	0.67	0.62	0.71
γ	0.81	0.71	0.57	0.75

r, β, and γ, although they differed between datasets, were of very similar magnitude for a given dataset analysed. Most datasets performed best in terms of r, related to event identification, as compared to β or γ, indicating that day-to-day variability between each dataset and the reference dataset was somewhat better matched than total precipitation amounts.

Even though the KGE performance indicator scores do not significantly differ between datasets, precipitation amounts, as well as trend magnitude and direction derived from these datasets deviate substantially from each other (Figure 4). The CHIRPS dataset most closely reproduces the GPCC trend patterns, with some areas of increases in annual precipitation across Mexico, significant drying in eastern Honduras and Nicaragua, and apparently drier conditions for most of the study area. By contrast, the ERA5, MERRA-2, and particularly the PERSIANN-CDR datasets, all of which diverge from the trends observed in the datasets more explicitly including station observations, mostly indicate increases in annual precipitation, especially in the southern portion of the study area, which overlaps with the summer and fall position of the Intertropical Convergence Zone. In addition, the MERRA-2 and PERSIANN-CDR datasets appear to generally underestimate precipitation amounts in the regions south of Mexico. Correspondingly, the mean annual precipitation between the first and the second half of the study period for the CHIRPS dataset significantly decreased by 10–25% for large areas of Honduras and Nicaragua (Figure 5), with areas of both increases and decreases in the remainder of the study period, while ERA5 and MERRA-2 indicate large increases in the region of the ITCZ, and statistically significant decreases in more northern regions, and PERSIANN-CDR suggests statistically significant increases of more than 25% for most of the study region. While an analysis of the teleconnections between ITCZ dynamics and regional rainfall is beyond the scope of this paper, it is interesting to note that better representation of the ITCZ has been associated with reduced precipitation biases over land (Cavazos *et al*., 2020). The closer agreement to CHIRPS of ERA-5 land precipitation

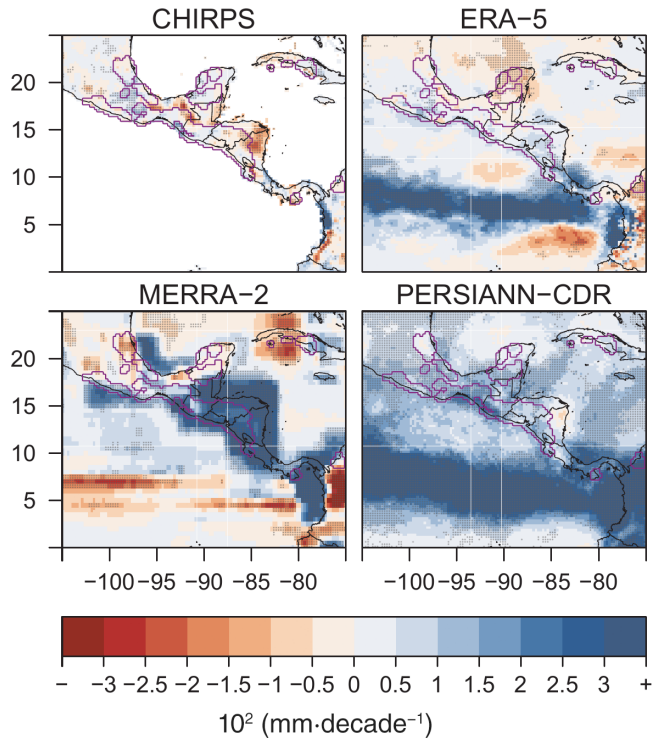

FIGURE 4 Trends in annual precipitation for the CHIRPS (1981–2019), ERA-5 (1981–2019), MERRA-2 (1981–2019), and PERSIANN-CDR (1983–2016) datasets examined in this study. Statistically significant areas marked with dark shading. Magenta boundaries indicate the delimitation of vulnerable regions developed by this study [Colour figure can be viewed at wileyonlinelibrary.com]

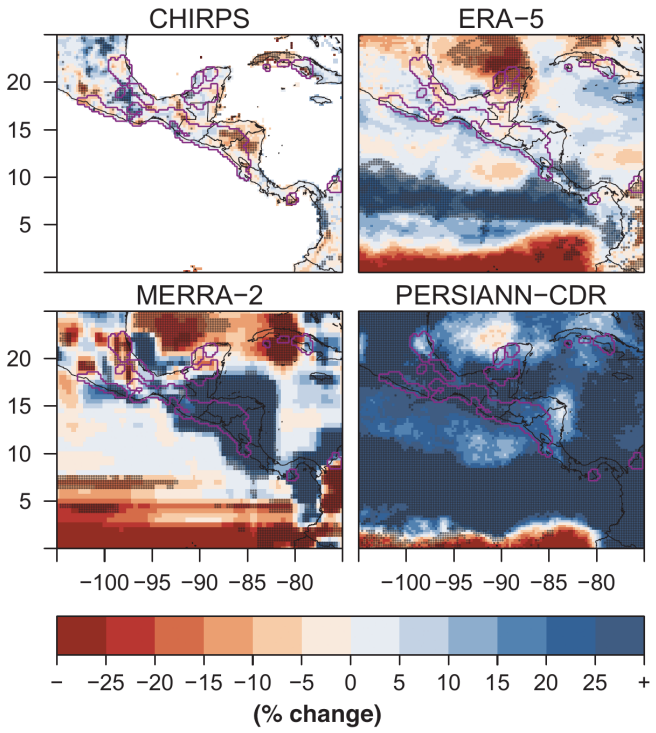

FIGURE 5 Percentage change in mean annual water availability between the first (1981–1999) and the second (2000–2019) half of the study period for the precipitation datasets evaluated. Significance in the means evaluated by the Wilcox test at the 95% confidence level indicated by darker shading. Magenta boundaries indicate the delimitation of vulnerable regions developed by this study [Colour figure can be viewed at wileyonlinelibrary.com]

trends compared to MERRA-2 and PERSIANN-CDR (Figures 4 and 5) also corresponds to MERRA-2 and PERSIANN-CDR showing greatly diverging precipitation trends in the ITCZ. The mean and standard deviation of annual precipitation trends within the climate sensitive regions shown in Figure 4 are −0.17(4.55)/1.39 (4.95)/12.54(14.46)/11.16(5.62) mm·year^{-1} for the CHIRPS/ERA-5/MERRA-2/PERSIANN-CDR datasets, respectively.

Similar to other global regions, trends in mean annual surface temperatures are more spatially coherent and consistent between datasets than those of annual precipitation (Figure 6). Mostly significant rises range between 0.2 and 0.8°C·decade^{-1}. Both the CHIRTS dataset, which incorporates ERA-5 data, and ERA-5 are in agreement of a general warming trend for the region. MERRA-2 suggests cooling over an area that includes Guatemala, Honduras, El Salvador, and Nicaragua. The rise in temperature suggested by the CHIRTS and ERA-5 corresponds to an overall warming of 0.8–3.2°C over the past four decades, raising the question whether this warming has been sufficient to contribute to significant increases in aridity.

While annual trends in precipitation are inconsistent across datasets and a large part of the study region, there is much greater consistency in seasonal changes between datasets (Figure 7 and Supporting Information). Seasonal trends indicate agreement between the CHIRPS, GPCC, the ERA5, and to some degree the MERRA-2 dataset for statistically significant drying during the summer season. The areas most affected by this drying are mostly to the north and east of the core region of the climate-sensitive area that stretches from southern Mexico to northwestern Costa Rica, but overlap between areas of summer drying, the climate-sensitive region determined by this study, as well as the CADC area determined by Quesada-Hernandez *et al*. (2019) does exist. Notably, even though ERA5 and MERRA-2 generally do not show reductions in annual water availability, these datasets do indicate drying during the summer growing season in some areas. The greatest increases in seasonal temperature have taken place in the winter and spring seasons for the

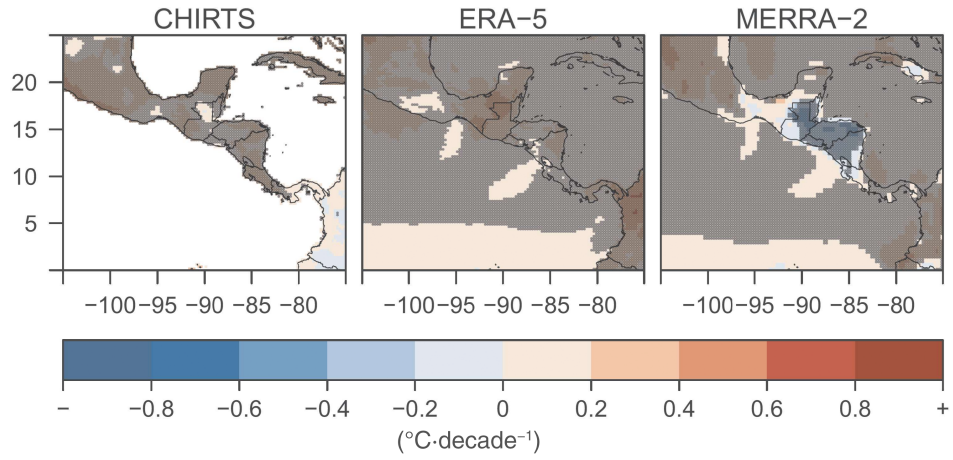

FIGURE 6 Trends in annual mean daily temperature (°C·decade^{-1}) for the CHIRTS (1983–2016), ERA5 (1981–2019), and MERRA-2 (1981–2019) datasets. Significant trends at the 95% confidence level are marked with dark shading [Colour figure can be viewed at wileyonlinelibrary.com]

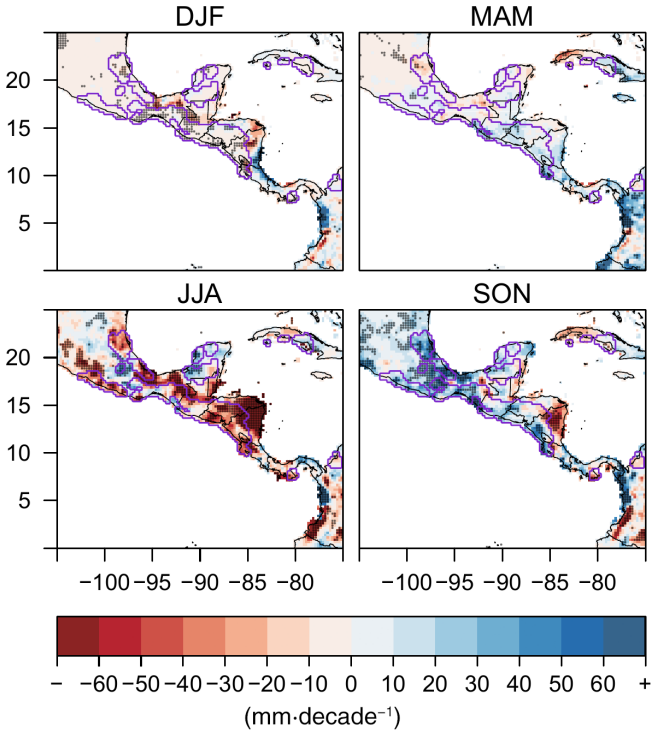

FIGURE 7 Seasonal precipitation trends for the CHIRPS dataset and the 1981–2019 period. Dark shading indicates significant trends at the 5% level. Magenta boundaries indicate the delimitation of vulnerable regions developed by this study [Colour figure can be viewed at wileyonlinelibrary.com]

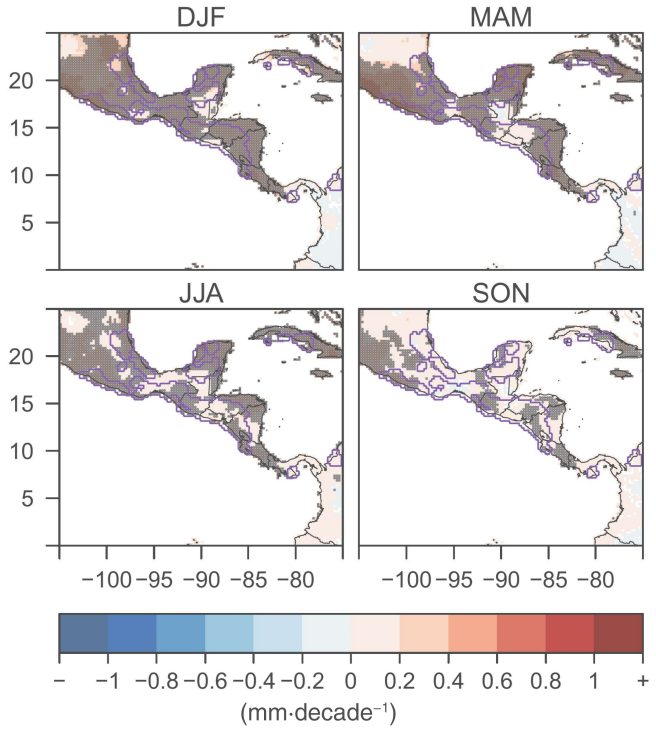

FIGURE 8 Seasonal trends (°C·decade^{-1}) in temperature for the CHIRTS dataset and the 1981–2016 period. Magenta boundaries indicate the delimitation of vulnerable regions developed by this study [Colour figure can be viewed at wileyonlinelibrary.com]

northern portion of the study region, particularly affecting Mexico and Cuba (Figure 8).

Consistent with the evidence from precipitation and temperature trends reported above, increases in DD_{SPI} and DD_{SPEI} are most pronounced for large regions of Honduras and Nicaragua, and smaller areas in Mexico during the midsummer drought months of July–August (Figure 9). Almost no parts of the study region appear to have experienced decreases in drought days during the growing season over the study period. For the drier portion of the year (November–April) few significant trends towards either increases or decreases in the number of drought days are found, with smaller regions of drier conditions mostly in the northern part of the study area, and areas of decreasing drought occurrence in the southern and Pacific side of the study area. Since SPEI includes the effects of temperature, and given the highly significant temperature trends in the region over the study period, it might be expected that increases in DD_{SPEI} would be

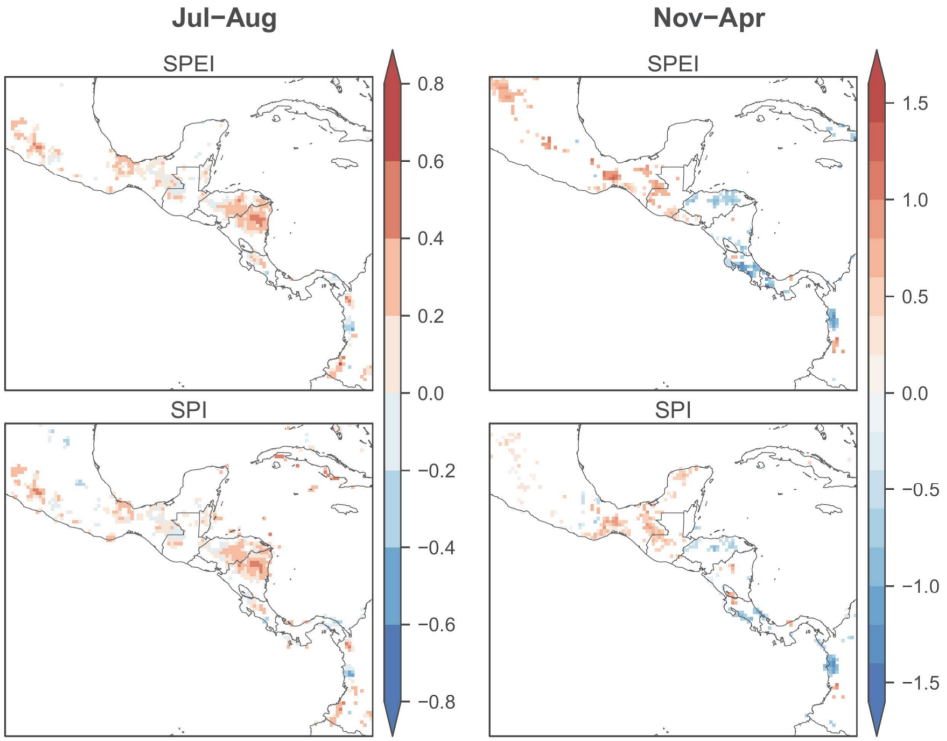

FIGURE 9 Trend (days·year^{-1}) in number of days with 31-day SPEI/SPI drought index values below −1 (DD_{SPI} and DD_{SPEI}) for the wet (Jul–Aug) and dry (Nov–Apr) seasons and the 1981–2019 period. Values based on daily CHIRPS precipitation and daily temperature from ERA5. Only grid cells with statistically significant trends are included [Colour figure can be viewed at wileyonlinelibrary.com]

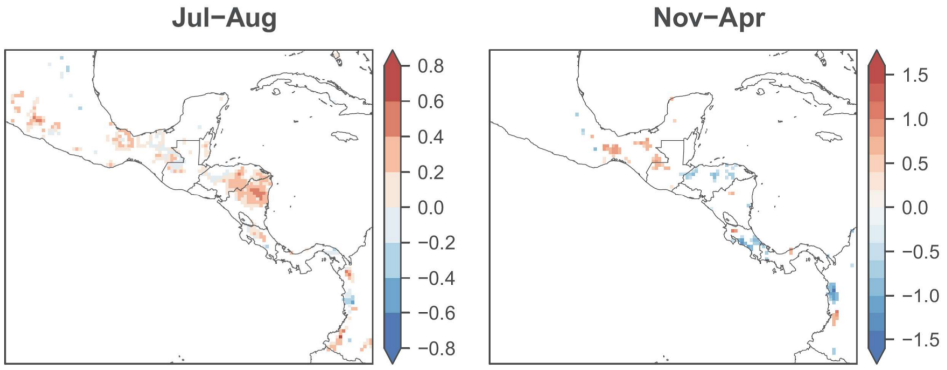

FIGURE 10 The same 31-day DD_{SPEI} trends (days·year^{-1}) as in Figure 9, except that detrended temperature was used for calculation. SPEI values below −1 are based on daily CHIRPS precipitation and daily detrended temperature from ERA-5 for the 1981–2018 period. Only grid cells with statistically significant trends are shown [Colour figure can be viewed at wileyonlinelibrary.com]

more severe as compared to the DD_{SPI}. However, the spatial extent and magnitude of statistically significant trends towards drying for both indices are nearly indistinguishable for the wetter July–August, and generally similar for the drier November–April season. Areas where DD_{SPI} and DD_{SPEI} for July–August increase partially aligns with the zone of the CADC as determined by Quesada-Hernandez *et al.* (2019) and the climate-sensitive region identified in this study.

The implication of the similarity in trends in DD_{SPI} and DD_{SPEI} is that the precipitation trends (especially drying trends) are driving the increases in July–August drought days more so than temperature, and hence PET, trends. A comparison of the SPEI trends in Figure 9 with those where temperature trends were removed (Figure 10) confirms this finding. When the temperature is detrended, the trends in the number of drought days according to SPEI values are comparatively similar between Figures 9 and 10. A summary of the number of grid cells showing significant trends in SPEI for each of the panels in Figures 9 and 10 is shown in Table 3.

For the July–August rainy season with the characteristic mid-summer drought in much of the region, the rising temperatures of the region for 1981–2018 account for a drop from 18.6 to 16.5% in the area with statistically significant trends, or stated differently, there is approximately a 12% increase in the number of significant trends when temperature trends are included. For July–August, in most locations the magnitude of the change in drought days due to temperature trends is generally small compared to the trend caused by decreasing precipitation. For the dry season (November–April) including the observed temperature trend for 1981–2018 increases the area with significant

TABLE 3 Percentage of significant grid cell trends in the number of SPEI drought days

	Jul–Aug	Nov–Apr
Original data (Figure 9)	18.6	11.7
Detrended data (Figure 10)	16.5	5.0

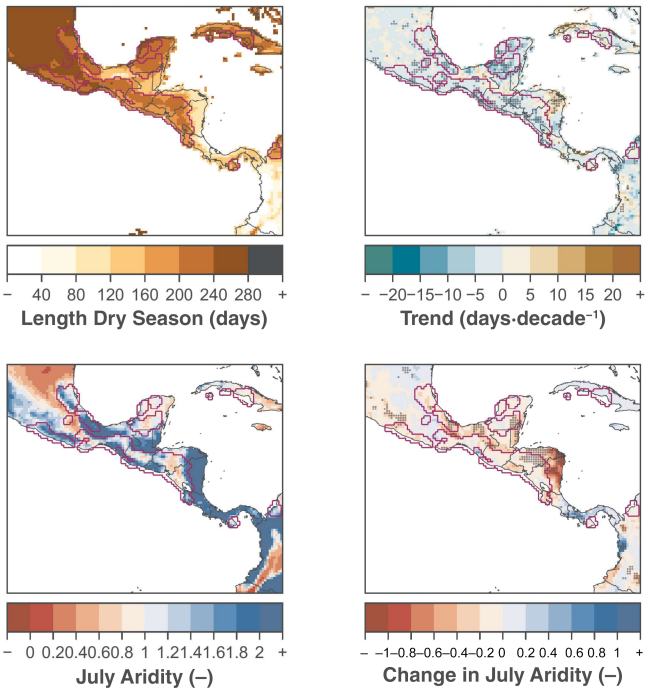

FIGURE 11 Top left: Maximum length of consecutive dry days, where dry is defined as <2.5 mm of precipitation on twice smoothed data. Top right: Trends in the length of consecutive dry days. Bottom left: Mean aridity for July and the 1981–1999 period. Bottom right: Difference in aridity between the (2000–2018) and (1981–1999) periods. Significant trends/changes at the 5% level are marked with dark shading [Colour figure can be viewed at wileyonlinelibrary.com]

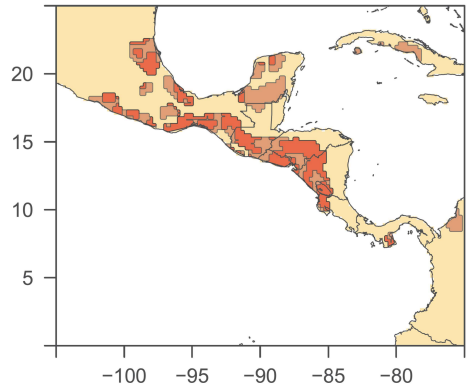

FIGURE 12 Climate sensitive regions as identified by this study (brown) and the areas within climate sensitive regions for which statistically significant trends towards drying in either mean annual precipitation, summer wet season (JJA) precipitation, winter dry season (DJF) precipitation, or July aridity were found indicated in red [Colour figure can be viewed at wileyonlinelibrary.com]

trends in drought days from 7.6 to 12.7% a 2/3 increase in area. This illustrates that temperatures are driving changes towards higher frequency in drought during the dry season for some locations, especially evident in portions of Mexico where Figure 9 shows significant drought day trends that are absent in Figure 10.

Extended dry periods of 4–8 months are prevalent in the northern and Pacific-side areas of the study region, especially for the higher elevations of Mexico, Guatemala, Honduras, El Salvador, and Nicaragua, and throughout Cuba (Figure 11). There is indication that the length of the dry period, L_{DS}, has shortened by 5–20 days on the Pacific side of Guatemala, Honduras, and Nicaragua in areas that overlap with vulnerable areas and in the Campeche region of Mexico, while increases in L_{DS} of 10–20 days were found for western Cuba, northern and northeastern Nicaragua, and eastern Honduras.

Even though the summer season is critical for replenishing water storage and agricultural production, there are substantial areas that remain water limited during that critical time (reddish colours in the lower left panel of Figure 11). July is also the month when changes in the aridity (AI) towards dryer conditions were found throughout the study area, with the largest and significant changes in eastern Honduras and Nicaragua (lower right panel of Figure 11).

A large fraction (approximately 60%) of the climate-sensitive regions identified in this study has been subject to statistically significant drying by at least one measure (Figure 12). The largest share of these areas lies along the Pacific coast of the isthmus.

4 | DISCUSSION

Throughout CA, rain-fed smallholder agriculture composes a large share of agricultural production and is highly sensitive to climatic variability on multiple temporal scales (Baca *et al.*, 2014; Bouroncle *et al.*, 2017). Decadal-scale warming and/or wetting/drying trends influence the viability and profitability of crop types or strains and drive management decisions for annual and perennial crops. Shorter term variability, such as variations in the start date and the length of either dry or rainy periods, the amount of water available in a season, or the interplay between temperature, precipitation, and thus evapotranspiration, impact crop successes, food security, and drinking and irrigation water resources on seasonal

to annual time scales. Despite the importance of precipitation timing and amounts for water and food security, much is uncertain about the direction and magnitude of recent climatic shifts in the region, owing to both the geographic complexity of the region and the lack of comprehensive on-the ground monitoring data (Aguilar *et al*., 2005; Muñoz-Jiménez *et al*., 2019; Quesada-Hernandez *et al*., 2019; Alfaro-Córdoba *et al*., 2020). As a result, satellite rainfall estimates have been used as an alternative or as a supplement to station observations in other regions worldwide, but Central America has not been a focus of these studies.

To fill this gap, our first objective was to evaluate the performance of several satellite and reanalysis precipitation data products for CA, referenced against the observation-based GPCC dataset. The data products were selected based on their strong performance elsewhere (Sun *et al*., 2018; Beck *et al*., 2019; Prakash, 2019). We found best performance across CA by the CHIRPS dataset, consistent with results from other regions in the lower latitudes (Dinku *et al*., 2018; Prakash, 2019), but in contrast to findings from mid-latitude regions, where MERRA-2 and ERA-5 outperformed the CHIRPS dataset (Beck *et al*., 2019). In agreement with prior work (Sun *et al*., 2018), all datasets performed better for the northern part of the study region that is less affected by the ITCZ and whose larger landmasses are less controlled by the Atlantic and Pacific Ocean systems. Nonetheless, the relative contribution of better station coverage, greater station overlap between datasets, or more stable climate systems over larger land areas to the better performance of datasets in the northern latitudes of CA remains unclear. Many satellite-based rainfall products with long time series suffer from coarse spatial and temporal resolutions and inhomogeneities. Thus, representing the broader CA region with its complex topography, where rain detection is inhibited, and its highly seasonal systems with difficult-to-detect light rains, remains a formidable challenge for all satellite products (Maggioni *et al*., 2016), which might necessitate the use of high resolution reanalysis data for the region.

Overall, our study identified only relatively small differences in performance metrics between datasets. By contrast, though, the hydroclimatic shifts calculated from each of the data products vary substantially. For temperature, the CHIRTS and ERA5 datasets are in agreement on widespread and significant warming over the entire study region, while the MERRA-2 indicates cooling has occurred over the central portion of the study period with warming elsewhere. By contrast, for precipitation, the reference dataset GPCC and CHIRPS, and to some degree ERA-5 appear to be mostly aligned, while MERRA-2 and PERSIANN-CDR products appear to be dominated by larger-scale oceanic processes. Those discrepancies have been reported elsewhere in the literature (e.g., Reichle *et al*., 2017a) who found that in regions where the density of gauge networks is low or where considerable changes in the network over the reanalysis period has taken place, MERRA-2 precipitation estimates are subject to considerable errors. While gauge undercatch has been noted as an issue in GPCC precipitation (Schneider *et al*., 2017), this influence is minor in tropical regions due to the absence of solid precipitation (Adam and Lettenmaier, 2003).

Our second objective sought to quantify hydroclimatic trends for the region based on the most recent and highest-performing data. For temperature, widespread warming trends on the order of $0.8°C \cdot decade^{-1}$, suggested by several the global temperature products evaluated in this study, are of serious concern in light of the importance of climate and agricultural production for smallholder livelihoods throughout the greater CA region. The patterns of warmer temperatures are consistent with those from previous studies for earlier periods (Hidalgo *et al*., 2015) and more recent warming for other regions worldwide (Shukla *et al*., 2020).

Similar to previous studies (Hannah *et al*., 2017; Muñoz-Jiménez *et al*., 2019; Sandonis *et al*., 2021), decadal-scale trends in annual precipitation were found to be more variable across the study region. They also differed in both direction and magnitude between the CHIRPS and GPCC datasets, and other satellite and reanalysis products. CHIRPS and GPCC found substantial declines in precipitation of 10–25% for a region centred on southern Honduras and northern Nicaragua, and trends towards declining annual precipitation in eastern Nicaragua and Honduras, and smaller regions in Mexico, while ERA-5 indicated declines for a region centred on the Yucatan in Mexico. By contrast, MERRA-2 and PERSIANN-CDR suggest >25% increases in annual totals over much of the study region. On sub-annual time scales, there is noteworthy agreement between datasets on much more widespread decreases in precipitation for the JJA boreal summer (wet) season. Historically, the wet season is most critical for food production, especially over regions with less annual precipitation and longer dry seasons. This suggests greater confidence in the detected drying trends during the main growing season for the more vulnerable parts of the study region. Unlike studies based on longer time periods (i.e., Sandonis *et al*., 2021), the 40-year record of satellite data available for this study was not sufficient to examine changes in the magnitudes of trends over time.

On annual time scales, measures of change in drought and aridity indicate substantial variability throughout the study region. Statistically significant

changes towards more frequent drought are only indicated for areas in southern Honduras, northern and eastern Nicaragua, and some smaller regions in Mexico, with few significant changes elsewhere. The length of the dry season, often exceeding 4 months throughout the study region, appears to be somewhat shortening through most of CA. On seasonal scales, our findings indicate greater frequency of drought and more arid conditions during the time of boreal summer (JJA). In addition, some highly seasonal, water-limited areas have seen significant increases in aridity during the summer through both increases in temperature and decreases in precipitation.

In line with precipitation trends, the most robust changes in summer drought observed were in the eastern Honduras/Nicaragua region as well as some areas of Mexico. For the 1981–2018 period, summer drought trends are driven almost entirely by precipitation, and not by warmer temperatures and associated increases in evapotranspiration. By the end of the century, runoff across CA is projected to decrease substantially due to rising temperatures (Imbach *et al*., 2017). Under recent warming, however, temperature trends add to increasing drought trends in some isolated regions but precipitation trends still dominate for most of the study region. As temperatures rise through the 21st century, the contributions to drought severity can be expected to change (Alfaro-Córdoba *et al*., 2020).

Despite the importance of both longer-term climatic changes and shorter-term variability, the characterization of recent hydroclimatic trends across CA likely contains significant uncertainties due to the paucity of available data and the geographic as well as the climatic complexity of the region. This complexity is not well represented at the larger spatial scales at which global models operate. Observed station data that provided the basis of previous publications relies on a set of station data that covers almost exclusively the Pacific side of the isthmus and has not been available past 1999. Thus reliance on global data products derived from a combination of satellite observations, reanalysis, and ground observations are critical for assessing climatic variability and change. As the hydroclimatic changes and drought over the past four decades have been driven by precipitation changes more so than to rising temperatures and greater evaporative demand, improved precipitation estimates would be even more important.

Based on the third objective for this study we determined areas of high climatic sensitivity following the characterizations for the Central American Dry Corridor (CADC). The CADC has been defined by bioregions, climatic characteristics, socio-economic vulnerability, susceptibility to drought, and a combination of these. Our work provides a delineation of climate-sensitive regions based on a 2019 consensus statement by practitioners in the field (Gotlieb *et al*., 2019) and applies this to the entire study region. Thus, our climate sensitive region, in contrast to previous delimitations, includes areas in Mexico, Cuba, and Columbia, and differs from a delineation derived from drought susceptibility (Quesada-Hernandez *et al*., 2019). Conceptually then, the regions identified by our delimitation are those where lower precipitation and high seasonality predominate, and for which drying may be particularly impactful. By contrast, Quesada-Hernandez *et al*. (2019) identify drought sensitive areas in the core CA region only, thus including areas of relative wetness, but excluding some water limited and highly seasonal areas that did not exhibit recent sensitivity to drought. While the largest drying in CA appears to have taken place in the wetter Atlantic regions of Honduras and Nicaragua, some areas inside the delimitation of climate sensitive areas have seen significant reductions in water availability. These climate sensitive areas are already highly vulnerable to precipitation reductions at the beginning of the study period, due to the limited rainfall and extreme seasonality present. Any changes towards even drier conditions in these regions would be particularly perilous.

5 | CONCLUSION

Despite the variability in precipitation changes in the region and the uncertainties associated with estimates from large-scale data products, two key findings emerge from our work. First, our study found that much of the decrease in water availability observed in the study region has been taking place during the summer wet season, a critical time for agricultural production. This is especially important in the later part of summer, when a second crop of staple foods might be successful in years with robust late rains. The decrease of the rains during this critical time points towards diminished opportunities for food production before the arrival for the annual dry period and is thus an important link of water and food security. Furthermore, when taken together, a large percentage of climate sensitive and water limited regions across CA have already experienced statistically significant increases in drought stress by one or more measures (decline in annual or seasonal precipitation, or an increase in aridity) over the past decades. These areas, mostly located in Nicaragua, Honduras, Mexico, Cuba, and Colombia are especially vulnerable to continuing changes towards drought and should be considered as focus areas for climate adaptation measures. Thus our findings provide insights that may guide adaptation to climate warming and water deficits in the socio-economically vulnerable broader Central American (CA) region.

ACKNOWLEDGEMENTS

We gratefully acknowledge funding for this work from U.S. National Science Foundation Grant BCS-1539795, DFG (German Research Foundation) Grant STA 632/6-1, and the Freiburg Institute of Advanced Studies (FRIAS) at Freiburg University (Germany). The first author would like to thank the Faculty of the Environment and Natural Resources at the University of Freiburg for hosting her during a research sabbatical. Our understanding of the impacts of climate on smallholder livelihoods has benefited from discussions with director Raúl Díaz and coworkers at CII-ASDENIC in northern Nicaragua. We thank our anonymous reviewers for their comments, which have greatly improved this manuscript. Open Access funding enabled and organized by Projekt DEAL.

AUTHOR CONTRIBUTIONS

Iris Stewart: Conceptualization; data curation; formal analysis; funding acquisition; investigation; methodology; project administration; visualization; writing - original draft; writing-review & editing. **Edwin Maurer:** Conceptualization; data curation; formal analysis; funding acquisition; investigation; methodology; visualization; writing - original draft; writing-review & editing. **Kerstin Stahl:** Funding acquisition; investigation; methodology; writing - original draft. **Kenneth Joseph:** Investigation.

ORCID

Iris T. Stewart https://orcid.org/0000-0002-0232-2367
Edwin P. Maurer https://orcid.org/0000-0001-7134-487X
Kerstin Stahl https://orcid.org/0000-0002-2159-9441

REFERENCES

Adam, J.C. and Lettenmaier, D.P. (2003) Adjustment of global gridded precipitation for systematic bias. *Journal of Geophysical Research*, 108, 1–14.

Aguilar, E., Aguilar, E., Peterson, T.C., Ramirez Obando, P., Frutos, R., Retana, J.A., Solera, M., Soley, J., Gonzalez Garcia, I., Araujo, R.M., Rosa Santos, A., Valle, V.E., Brunet, M., Aguilar, L., Alvarez, L., Bautista, M., Castañon, C., Herrera, L., Ruano, E., Sinay, J.J., Sanchez, E., Hernandez Oviedo, G.I., Obed, F., Salgado, J.E., Vazquez, J.L., Baca, M., Gutierrez, M., Centella, C., Espinosa, J., Martinez, D., Olmedo, B., Ojeda Espinoza, C.E., Nuñez, R., Haylock, M., Benavides, H. and Mayorga, R. (2005) Changes in precipitation and temperature extremes in Central America and northern South America, 1961–2003. *Journal of Geophysical Research*, 110, D23107. https://doi.org/10.1029/2005JD006119.

Albergel, C., Dutra, E., Munier, S., Calvet, J.-C., Munoz-Sabater, J., de Rosnay, P. and Balsamo, G. (2018) ERA-5 and ERA-Interim driven ISBA land surface model simulations: which one performs better? *Hydrology and Earth System Sciences*, 22, 3515–3532. https://doi.org/10.5194/hess-22-3515-2018.

Alfaro-Córdoba, M., Hidalgo, H.G. and Alfaro, E.J. (2020) Aridity trends in Central America: a spatial correlation analysis. *Atmosphere*, 11, 427. https://doi.org/10.3390/atmos11040427.

Anderson, T.G., Anchukaitis, K.J., Pons, D. and Taylor, M. (2019) Multiscale trends and precipitation extremes in the Central American midsummer drought. *Environmental Research Letters*, 14(12), 124016.

Ashouri, H., Hsu, K.-L., Sorooshian, S., Braithwaite, D.K., Knapp, K.R., Cecil, L.D., Nelson, B.R. and Prat, O.P. (2015) PERSIANN-CDR: daily precipitation climate data record from multisatellite observations for hydrological and climate studies. *Bulletin of the American Meteorological Society*, 96, 69–83.

Ashouri, H., Nguyen, P., Thorstensen, A., Hsu, K., Sorooshian, S. and Braithwaite, D. (2016) Assessing the efficacy of high-resolution satellite-based PERSIANN-CDR precipitation product in simulating streamflow. *Journal of Hydrometeorology*, 17, 2061–2076.

Avelino, J., Cristancho, M., Georgiou, S., Imbach, P., Aguilar, L., Bornemann, G., Läderach, P., Anzueto, F., Hruska, A.J. and Morales, C. (2015) The coffee rust crises in Colombia and Central America (2008–2013): impacts, plausible causes and proposed solutions. *Food Security*, 7, 303–321. https://doi.org/10.1007/s12571-015-0446-9.

Baca, M., Läderach, P., Haggar, J., Schroth, G. and Ovalle, O. (2014) An integrated framework for assessing vulnerability to climate change and developing adaptation strategies for coffee growing families in Mesoamerica. *PLoS One*, 9, e88463. https://doi.org/10.1371/journal.pone.0088463.

Beck, H.E., Pan, M., Roy, T., Weedon, G.P., Pappenberger, F., van Dijk, A.I.J.M., Huffman, G.J., Adler, R.F. and Wood, E.F. (2019) Daily evaluation of 26 precipitation datasets using stage-IV gauge-radar data for the CONUS. *Hydrology and Earth System Sciences*, 23, 207–224. https://doi.org/10.5194/hess-23-207-2019.

Bennett, A.R., Hamman, J.J. and Nijssen, B. (2020) MetSim: a Python package for estimation and disaggregation of meteorological data. *Journal of Open Source Software*, 5, 2042. https://doi.org/10.21105/joss.02042.

Bouroncle, C., Imbach, P., Rodríguez-Sánchez, B., Medellín, C., Martinez-Valle, A. and Läderach, P. (2017) Mapping climate change adaptive capacity and vulnerability of smallholder agricultural livelihoods in Central America: ranking and descriptive approaches to support adaptation strategies. *Climatic Change*, 141, 123–137. https://doi.org/10.1007/s10584-016-1792-0.

Cabos, W., Sein, D.V., Durán-Quesada, A., Liguori, G., Koldunov, N.V., Martínez-López, B., Alvarez, F., Sieck, K., Limareva, N. and Pinto, J.G. (2019) Dynamical downscaling of historical climate over CORDEX Central America domain with a regionally coupled atmosphere–ocean model. *Climate Dynamics*, 52(7), 4305–4328.

Carvalho, L.M.V. (2020) Assessing precipitation trends in the Americas with historical data: a review. *WIREs Climate Change*, 11, e627. https://doi.org/10.1002/wcc.627.

Cavazos, T., Luna-Niño, R., Cerezo-Mota, R., Fuentes-Franco, R., Méndez, M., Pineda Martínez, L.F. and Valenzuela, E. (2020) Climatic trends and regional climate models intercomparison over the CORDEX-CAM (Central America, Caribbean, and Mexico) domain. *International Journal of Climatology*, 40, 1396–1420. https://doi.org/10.1002/joc.6276.

Chen, S., Liu, B., Tan, X. and Wu, Y. (2020) Inter-comparison of spatiotemporal features of precipitation extremes within six daily precipitation products. *Climate Dynamics*, 54, 1057–1076.

Copernicus Climate Change Service (C3S). (2017) *ERA5: Fifth generation of ECMWF atmospheric reanalyses of the global climate*. Copernicus Climate Change Service Climate Data Store (CDS). Available at: https://cds.climate.copernicus.eu/cdsapp#!/home [Accessed 20th February 2020].

Dinku, T., Funk, C., Peterson, P., Maidment, R., Tadesse, T., Gadain, H. and Ceccato, P. (2018) Validation of the CHIRPS satellite rainfall estimates over eastern Africa. *Quarterly Journal of the Royal Meteorological Society*, 144, 292–312. https://doi.org/10.1002/qj.3244.

Funk, C., Peterson, P., Landsfeld, M., Pedreros, D., Verdin, J., Shukla, S., Husak, G., Rowland, J., Harrison, L., Hoell, A. and Michaelsen, J. (2015) The climate hazards infrared precipitation with stations—a new environmental record for monitoring extremes. *Scientific Data*, 2(1), 1–21.

Funk, C., Peterson, P., Peterson, S., Shukla, S., Davenport, F., Michaelsen, J., Knapp, K.R., Landsfeld, M., Husak, G. and Harrison, L. (2019) A high-resolution 1983–2016 Tmax climate data record based on infrared temperatures and stations by the climate hazard center. *Journal of Climate*, 32, 5639–5658.

Funk, C.C., Peterson, P.J., Landsfeld, M.F., Pedreros, D.H., Verdin, J.P., Rowland, J.D., Romero, B.E., Husak, G.J., Michaelsen, J.C. and Verdin, A.P. (2014) A quasi-global precipitation time series for drought monitoring. In: *US Geological Survey Data Series*, Vol. 832. Reston, VA: USGS, pp. 1–12.

Gelaro, R., McCarty, W., Suárez, M.J., Todling, R., Molod, A., Takacs, L., Randles, C.A., Darmenov, A., Bosilovich, M.G. and Reichle, R. (2017) The modern-era retrospective analysis for research and applications, version 2 (MERRA-2). *Journal of Climate*, 30, 5419–5454.

Global Modeling and Assimilation Office (GMAO). (2015) *MERRA-2*. Greenbelt, MD: Goddard Earth Sciences Data and Information Services Center (GES DISC) Available at: https://doi.org/10.5067/0JRLVL8YV2Y4 [Accessed 11th May 2020].

Gotlieb, Y., Pérez-Briceño, P.M., Hidalgo, H.G. and Alfaro, E.J. (2019) The Central American dry corridor: a consensus statement and its background. *Revista Yu'am*, 3, 42–51.

Greve, P., Roderick, M.L., Ukkola, A.M. and Wada, Y. (2019) The aridity index under global warming. *Environmental Research Letters*, 14, 124006. https://doi.org/10.1088/1748-9326/ab5046.

Gupta, H.V., Kling, H., Yilmaz, K.K. and Martinez, G.F. (2009) Decomposition of the mean squared error and NSE performance criteria: implications for improving hydrological modelling. *Journal of Hydrology*, 377, 80–91.

Hanke, M., Redler, R., Holfeld, T. and Yastremsky, M. (2016) YAC 1.2. 0: new aspects for coupling software in Earth system modelling. *Geoscientific Model Development*, 9(8), 2755–2769.

Hannah, L., Donatti, C.I., Harvey, C.A., Alfaro, E., Rodriguez, D.A., Bouroncle, C., Castellanos, E., Diaz, F., Fung, E. and Hidalgo, H.G. (2017) Regional modeling of climate change impacts on smallholder agriculture and ecosystems in Central America. *Climatic Change*, 141, 29–45.

Harris, I., Osborn, T.J., Jones, P. and Lister, D. (2020) Version 4 of the CRU TS monthly high-resolution gridded multivariate climate dataset. *Scientific Data*, 7(1), 1–18.

Heim, R.R. (2002) A review of twentieth-century drought indices used in the United States. *Bulletin of the American Meteorological Society*, 83, 1149–1166. https://doi.org/10.1175/1520-0477-83.8.1149.

Hersbach, H., Bell, B., Berrisford, P., Hirahara, S., Horányi, A., Muñoz-Sabater, J., Nicolas, J., Peubey, C., Radu, R. and Schepers, D. (2020) The ERA5 global reanalysis. *Quarterly Journal of the Royal Meteorological Society*, 146, 1999–2049.

Hidalgo, H., Alfaro, E. and Quesada-montano, B. (2017) Observed (1970–1999) climate variability in Central America using a high-resolution meteorological dataset with implication to climate change studies. *Climatic Change*, 141, 13–28. https://doi.org/10.1007/s10584-016-1786-y.

Hidalgo, H.G., Amador, J.A., Alfaro, E.J. and Quesada, B. (2013) Hydrological climate change projections for Central America. *Journal of Hydrology*, 495, 94–112.

Hidalgo, H.G., Durán-Quesada, A.M., Amador, J.A. and Alfaro, E.J. (2015) The caribbean low-level jet, the inter-tropical convergence zone and precipitation patterns in the intra-americas sea: a proposed dynamical mechanism. *Geografiska Annaler: Series A, Physical Geography*, 97, 41–59.

Imbach, P., Beardsley, M., Bouroncle, C., Medellin, C., Läderach, P., Hidalgo, H., Alfaro, E., Van Etten, J., Allan, R., Hemming, D., Stone, R., Hannah, L. and Donatti, C.I. (2017) Climate change, ecosystems and smallholder agriculture in Central America: an introduction to the special issue. *Climatic Change*, 141, 1–12. https://doi.org/10.1007/s10584-017-1920-5.

Jones, P.W. (1999) First-and second-order conservative remapping schemes for grids in spherical coordinates. *Monthly Weather Review*, 127(9), 2204–2210.

Karmalkar, A.V., Bradley, R.S. and Diaz, H.F. (2011) Climate change in Central America and Mexico: regional climate model validation and climate change projections. *Climate Dynamics*, 37(3–4), 605.

Kendall, M.G. (1948) *Rank Correlation Methods*. London: Springer.

Kimball, J.S., Running, S.W. and Nemani, R. (1997) An improved method for estimating surface humidity from daily minimum temperature. *Agricultural and Forest Meteorology*, 85, 87–98. https://doi.org/10.1016/S0168-1923(96)02366-0.

Kling, H., Fuchs, M. and Paulin, M. (2012) Runoff conditions in the upper Danube basin under an ensemble of climate change scenarios. *Journal of Hydrology*, 424, 264–277.

Kreft, S., Eckstein, D. and Melchior, I. (2013) Who suffers most from extreme weather events? Weather-related loss events in 2019 and 2000 to 2019. In: *Global Climate Risk Index 2014*. Bonn: Germanwatch.

Liu, X., Liu, B., Henderson, M., Xu, M. and Zhou, D. (2015) Observed changes in dry day frequency and prolonged dry episodes in Northeast China. *International Journal of Climatology*, 35, 196–214. https://doi.org/10.1002/joc.3972.

Magaña, V., Amador, J.A. and Medina, S. (1999) The midsummer drought over Mexico and Central America. *Journal of Climate*, 12, 1577–1588.

Maggioni, V., Meyers, P.C. and Robinson, M.D. (2016) A review of merged high-resolution satellite precipitation product accuracy during the Tropical Rainfall Measuring Mission (TRMM) era. *Journal of Hydrometeorology*, 17, 1101–1117. https://doi.org/10.1175/JHM-D-15-0190.1.

Maldonado, T., Alfaro, E.J. and Hidalgo, H.G. (2018) A review of the main drivers and variability of Central America's climate

and seasonal forecast systems. *Revista de Biología Tropical*, 66, S153–S175.

Mann, H.B. (1945) Nonparametric tests against trend. *Econometrica*, 13, 245–259.

Marvel, K., Cook, B.I., Bonfils, C.J., Durack, P.J., Smerdon, J.E. and Williams, A.P. (2019) Twentieth-century hydroclimate changes consistent with human influence. *Nature*, 569, 59–65.

McCabe, G.J., Legates, D.R. and Lins, H.F. (2010) Variability and trends in dry day frequency and dry event length in the southwestern United States. *Journal of Geophysical Research: Atmospheres*, 115, D07108. https://doi.org/10.1029/2009JD012866.

McKee, T.B., Doesken, N.J., and Kleist, J. (1993) *The relationship of drought frequency and duration to time scales*. Paper presented at Eighth Conference on Applied Climatology, January 17–22, 1993, Anaheim, California.

Mesinger, F., DiMego, G., Kalnay, E., Mitchell, K., Shafran, P.C., Ebisuzaki, W., Jović, D., Woollen, J., Rogers, E., Berbery, E.H., Ek, M.B., Fan, Y., Grumbine, R., Higgins, W., Li, H., Lin, Y., Manikin, G., Parrish, D. and Shi, W. (2006) North American regional reanalysis. *Bulletin of the American Meteorological Society*, 87(3), 343–360.

Mirzabaev, A., Wu, J., Evans, J., García-Oliva, F., Hussein, I.A.G., Iqbal, M.H., Kimutai, J., Knowles, T., Meza, F., Nedjraoui, D., Tena, F., Türkeş, M., Vázquez, R.J. and Weltz, M. (2019) Desertification. In: Shukla, P.R., Skea, J., Buendia, E.C., Masson-Delmotte, V., Pörtner, H.-O., Roberts, D.C., Zhai, P., Slade, R., Connors, S., van Diemen, R., Ferrat, M., Haughey, E., Luz, S., Neogi, S., Pathak, M., Petzold, J., Pereira, J.P., Vyas, P., Huntley, E., Kissick, K., Belkacemi, M. and Malley, J. (Eds.) *Climate Change and Land: An IPCC Special Report on Climate Change, Desertification, Land Degradation, Sustainable Land Management, Food Security, and Greenhouse Gas Fluxes in Terrestrial Ecosystems*. Geneva: IPCC.

Muñoz-Jiménez, R., Giraldo-Osorio, J.D., Brenes-Torres, A., Avendaño-Flores, I., Nauditt, A., Hidalgo-León, H.G. and Birkel, C. (2019) Spatial and temporal patterns, trends and teleconnection of cumulative rainfall deficits across Central America. *International Journal of Climatology*, 39, 1940–1953.

NOAA National Centers for Environmental Information. (2020) *State of the climate: Global climate report for July 2020*. Availabble at: https://www.ncdc.noaa.gov/sotc/global/202007 [Accessed September 15, 2020].

Nogueira, M. (2020) Inter-comparison of ERA-5, ERA-interim and GPCP rainfall over the last 40 years: process-based analysis of systematic and random differences. *Journal of Hydrology*, 583, 124632. https://doi.org/10.1016/j.jhydrol.2020.124632.

Pennington, R.T. and Ratter, J.A. (2006) *Neotropical Savannas and Seasonally Dry Forests: Plant Diversity, Biogeography, and Conservation*. Boca Raton: CRC Press.

Pérez-Briceño, P.M., Alfaro, E.J., Hidalgo, H.G. and Jiménez, F. (2016) Distribución espacial de impactos de eventos hidrometeorológicos en América Central. *Revista de Climatologia*, 16, 63–75.

Peterson, P., Funk, C.C., Landsfeld, M.F., Pedreros, D.H., Shukla, S., Husak, G.J., Harrison, L. and Verdin, J.P. (2015) The climate hazards group infrared precipitation with stations (CHIRPS) v2.0 dataset: 35 year quasi-global precipitation estimates for drought monitoring. *AGU Fall Meeting*, 2015, NH41D-05.

Prakash, S. (2019) Performance assessment of CHIRPS, MSWEP, SM2RAIN-CCI, and TMPA precipitation products across India. *Journal of Hydrology*, 571, 50–59. https://doi.org/10.1016/j.jhydrol.2019.01.036.

Quesada-Hernandez, L.E., Calvo-Solano, O.D., Hidalgo, H.G., Perez-Briceno, P.M. and Alfaro, E.J. (2019) Dynamical delimitation of the Central American Dry Corridor (CADC) using drought indices and aridity values. *Progress in Physical Geography: Earth and Environment*, 43, 627–642.

Reichle, R.H., Draper, C.S., Liu, Q., Girotto, M., Mahanama, S.P., Koster, R.D. and De Lannoy, G.J. (2017a) Assessment of MERRA-2 land surface hydrology estimates. *Journal of Climate*, 30, 2937–2960.

Reichle, R.H., Liu, Q., Koster, R.D., Draper, C.S., Mahanama, S.P. and Partyka, G.S. (2017b) Land surface precipitation in MERRA-2. *Journal of Climate*, 30, 1643–1664.

ReliefWeb. (2020) *Central America: drought 2014–2017*. Available at: https://reliefweb.int/disaster/dr-2014-000132-hnd [Accessed January 9, 2020].

Sandonis, L., González-Hidalgo, J.C., Peña-Angulo, D. and Beguería, S. (2021) Mean temperature evolution on the Spanish mainland 1916–2015. *Climate Research*, 82, 177–189.

Schneider, U., Becker, A., Finger, P., Meyer-Christoffer, A. and Ziese, M. (2018) *GPCC monitoring product: near real-time monthly land-surface precipitation from rain-gauges based on SYNOP and CLIMAT data*. Offenbach: Deutscher Wetterdienst.

Schneider, U., Finger, P., Meyer-Christoffer, A., Rustemeier, E., Ziese, M. and Becker, A. (2017) Evaluating the hydrological cycle over land using the newly-corrected precipitation climatology from the Global Precipitation Climatology Centre (GPCC). *Atmosphere*, 8, 52.

Sen, P.K. (1968) Estimates of the regression coefficient based on Kendall's tau. *Journal of the American Statistical Association*, 63, 1379–1389.

Shukla, P.R., Skea, J., Slade, R., van Diemen, R., Haughey, E., Malley, J., Pathak, M. and Portugal Pereira, J. (2020) *Climate Change and Land: An IPCC Special Report on Climate Change, Desertification, Land Degradation, Sustainable Land Management, Food Security, and Greenhouse Gas Fluxes in Terrestrial Ecosystems*. Geneva: IPCC.

Siegel, A.F. (1982) Robust regression using repeated medians. *Biometrika*, 69, 242–244.

Soroosh, S., Kuolin, H., Dan, B., Hamed, A. and NOAA CDR Program. (2014) *NOAA climate data record (CDR) of precipitation estimation from remotely sensed information using artificial neural networks (PERSIANN-CDR)*. NOAA National Centers for Environmental Information. Available at: https://doi.org/10.7289/V51V5BWQ [Accessed 26th June 2020].

Stagge, J.H., Tallaksen, L.M., Gudmundsson, L., Loon, A.F.V. and Stahl, K. (2015) Candidate distributions for climatological drought indices (SPI and SPEI). *International Journal of Climatology*, 35, 4027–4040. https://doi.org/10.1002/joc.4267.

Sun, Q., Miao, C., Duan, Q., Ashouri, H., Sorooshian, S. and Hsu, K. (2018) A review of global precipitation data sets: data sources, estimation, and intercomparisons. *Reviews of Geophysics*, 56, 79–107.

Tang, G., Clark, M.P., Papalexiou, S.M., Ma, Z. and Hong, Y. (2020) Have satellite precipitation products improved over last two decades? A comprehensive comparison of GPM IMERG with

nine satellite and reanalysis datasets. *Remote Sensing of Environment*, 240, 111697. https://doi.org/10.1016/j.rse.2020.111697.

Thornton, P.E. and Running, S.W. (1999) An improved algorithm for estimating incident daily solar radiation from measurements of temperature, humidity, and precipitation. *Agricultural and Forest Meteorology*, 93, 211–228. https://doi.org/10.1016/S0168-1923(98)00126-9.

van der Zee Arias, A., van der Zee, J., Meyrat, A., Poveda, C. and Picado, L. (2012) Estudio de la caracterización del Corredor Seco Centroamericano. In: *Organización de las Naciones Unidas para la Alimentación y la Agricultura (FAO)*. Tegulcigalpa. The Food and Agriculture Organization,

Vicente-Serrano, S.M., Beguería, S. and López-Moreno, J.I. (2010) A multiscalar drought index sensitive to global warming: the standardized precipitation evapotranspiration index. *Journal of Climate*, 23, 1696–1718. https://doi.org/10.1175/2009JCLI2909.1.

Wani, S.P., Sreedevi, T.K., Rockström, J. and Ramakrishna, Y.S. (2009) *Rainfed agriculture–past trends and future prospects*. Rainfed agriculture: Unlocking the potential. CABI. 7, 1–33.

Wilcoxon, F. (1945) Individual comparisons by ranking methods. *Biometric Bulletin*, 1, 80–83. https://doi.org/10.2307/3001968.

Zhao, H. and Ma, Y. (2019) Evaluating the drought-monitoring utility of four satellite-based quantitative precipitation estimation products at global scale. *Remote Sensing*, 11, 2010. https://doi.org/10.3390/rs11172010.

Ziese, M., Rauthe-Schöch, A., Becker, A., Finger, P., Meyer-Christoffer, A. and Schneider, U. (2018) *GPCC full data daily version.2018 at 1.0°: daily land-surface precipitation from rain-gauges built on GTS-based and historic data*. Offenbach: Deutscher Wetterdienst.

SUPPORTING INFORMATION

Additional supporting information may be found online in the Supporting Information section at the end of this article.

How to cite this article: Stewart, I. T., Maurer, E. P., Stahl, K., & Joseph, K. (2022). Recent evidence for warmer and drier growing seasons in climate sensitive regions of Central America from multiple global datasets. *International Journal of Climatology*, *42*(3), 1399–1417. https://doi.org/10.1002/joc.7310